

## Mechanical and Corrosion Performance of the Weld of 740H and 282

**Andrew Brittan**  
Research Assistant  
University of Wisconsin-Madison  
Madison, WI, USA  
abrittan@wisc.edu

**Dr. Mark Anderson**  
Professor  
University of Wisconsin-Madison  
Madison, WI, USA  
manderson@engr.wisc.edu

**Dr. Jacob Mahaffey**  
Postdoctoral Researcher  
Sandia National Laboratory\*  
Albuquerque, NM, USA  
jtmahaf@sandia.gov

**Dr. Kumar Sridharan**  
Research Professor  
University of Wisconsin-Madison  
Madison, WI, USA  
kumar@engr.wisc.edu



*Andrew Brittan is a research assistant under Dr. Mark Anderson. His research focuses on strength of materials and welds in supercritical carbon dioxide environments. He attended the University of California Los Angeles where he received his BS in Mechanical Engineering in 2011.*



*Dr. Jacob Mahaffey received his PhD in Nuclear Engineering & Engineering Physics from the University of Wisconsin-Madison in 2017 under the advisement of Dr. Mark Anderson. His work at Wisconsin focused on the effects of the partial pressure of oxygen and carbon activity on the corrosion of high temperature alloys in supercritical CO<sub>2</sub> environments. After receiving his PhD, Jacob now works at Sandia National Laboratories as a postdoctoral researcher at the Thermal Spray Research Laboratory.*



*Dr. Mark Anderson is a professor in the Department of Mechanical Engineering and Director of the University of Wisconsin's Thermal Hydraulic Laboratory. He also manages the UW - Madison Tantalus facility in Stoughton WI. Dr. Anderson studies both the physics, thermal hydraulic performance and material corrosion issues of several different fluids (salts, liquid metals, SCW, sCO<sub>2</sub>).*



*Dr. Kumar Sridharan's expertise spans a broad spectrum of areas in materials science, including nuclear reactor materials, corrosion, physical metallurgy, surface modification and coatings processes, ion implantation, plasma-based synthesis and deposition of materials, characterization and testing of materials, interfaces of materials and manufacturing, and industrial applications*

\*Sandia National Laboratories is a multimission laboratory managed and operated by National Technology and Engineering Solutions of Sandia, LLC., a wholly owned subsidiary of Honeywell International, Inc., for the U.S. Department of Energy's National Nuclear Security Administration under contract DE-NA-0003525.

## ABSTRACT

The mechanical properties of INCONEL 740H and Haynes 282 and their similar welds were investigated after exposure in research grade (RG) CO<sub>2</sub> (99.999% pure) under supercritical (sCO<sub>2</sub>) conditions at 20MPa and 750°C for 1,000 hours. Welded samples were cut in the transverse direction with the fusion zone located in the gauge region. The tensile properties of both welded and base material of both alloys were determined pre-exposure and found to have results consistent with the manufacturers of the alloys, Special Metals and Haynes, respectively. In regard to 740H, exposure to sCO<sub>2</sub> on base material caused an increase in both ultimate tensile strength (UTS) and yield strength (YS) with a 30% decrease in elongation. In contrast, welded samples experienced a decrease in UTS, YS, and elongation. In the case of Haynes 282, exposure to sCO<sub>2</sub> resulted in only a moderate increase to YS, with no change to UTS and a 49% drop in elongation in the base material. Welded samples of Haynes 282 exhibited an increase in UTS and YS, with no change in elongation. Analysis of the corrosion behavior of welded samples of 740H and Haynes 282 exhibited a 23% and 34% higher mass gain than for the base material samples, respectively. Given that there was no observed spallation of the oxide, this indicated increased corrosion activity in the form of carbon and oxygen uptake. There is no evidence that carburization occurred in the bulk of these samples due to the CO<sub>2</sub> environment. It has been determined that exposure to the sCO<sub>2</sub> environment has very little effect on the macroscopic mechanical properties of either welded or base material samples apart from the heat treatment of the material during exposure. It is hypothesized that the welded samples experienced deterioration of macroscopic properties due to the larger grain size in the fusion zone enhancing the effect of the internal carbide formation.

## INTRODUCTION

Supercritical carbon dioxide (sCO<sub>2</sub>) is currently being considered as a working fluid for the Brayton cycle in next generation power systems for uses across nuclear, solar, and fossil power sources. The Brayton cycle has been found to produce higher efficiencies than the Rankine cycle at comparable operating temperatures. In addition, using CO<sub>2</sub> as working fluid has shown comparable efficiency to Helium at lower temperatures, through the advantage of the property changes of CO<sub>2</sub> near the critical point (Dostal, 2004). However, implementation of the sCO<sub>2</sub> Brayton cycle will not be possible without a thorough understanding of the effects of the environment on the candidate materials.

Nickel-base superalloys – such as INCONEL 740H (740H) and Haynes 282 (282) – are being considered for high temperature components due to their good corrosion resistance and mechanical properties at high temperatures. As seen in Figure 1, 740H has especially good strength at temperatures up to 800°C. Both 740H and 282 have also shown good corrosion resistance in research grade (RG) CO<sub>2</sub> (99.999% pure) in relation to other comparable alloys, as shown in Figure 2 (“Boiler and Pressure Vessel Code: Section II Part D,” 2013). Additionally, carburization has been seen to be extremely limited in nickel base alloys, with a maximum depth of only a few microns from the oxide in CO<sub>2</sub> at 750°C and 20MPa, so bulk material properties are not expected to be largely affected by the CO<sub>2</sub> environment (Mahaffey, 2017).

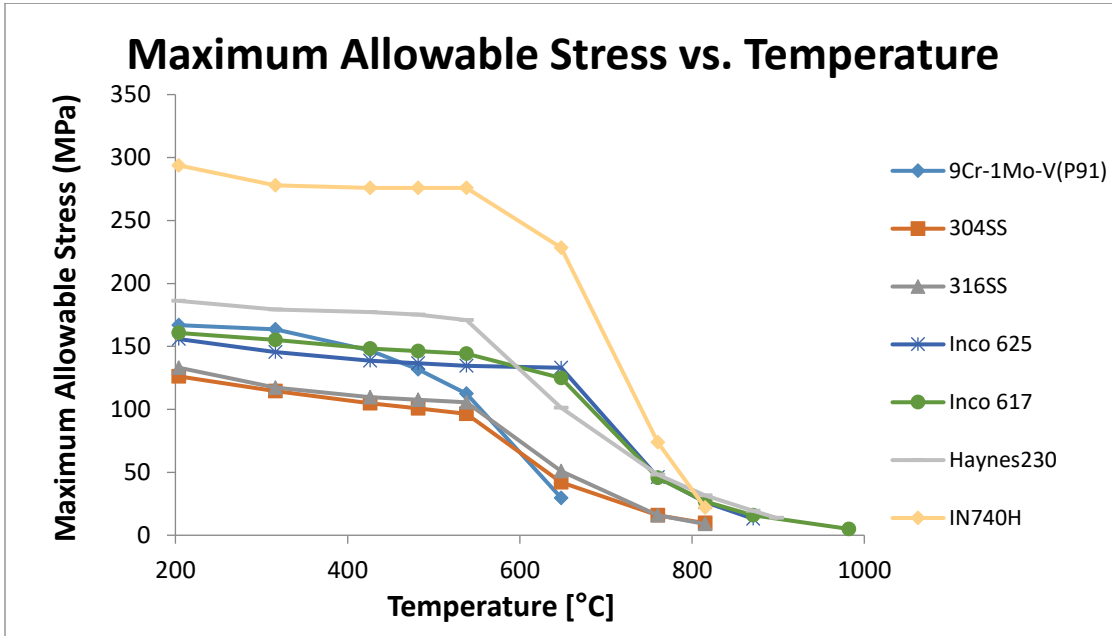


Figure 1 - Allowable stress vs. Temperature for INCONEL Alloys 617 and 740H (“Boiler and Pressure Vessel Code: Section II Part D,” 2013)

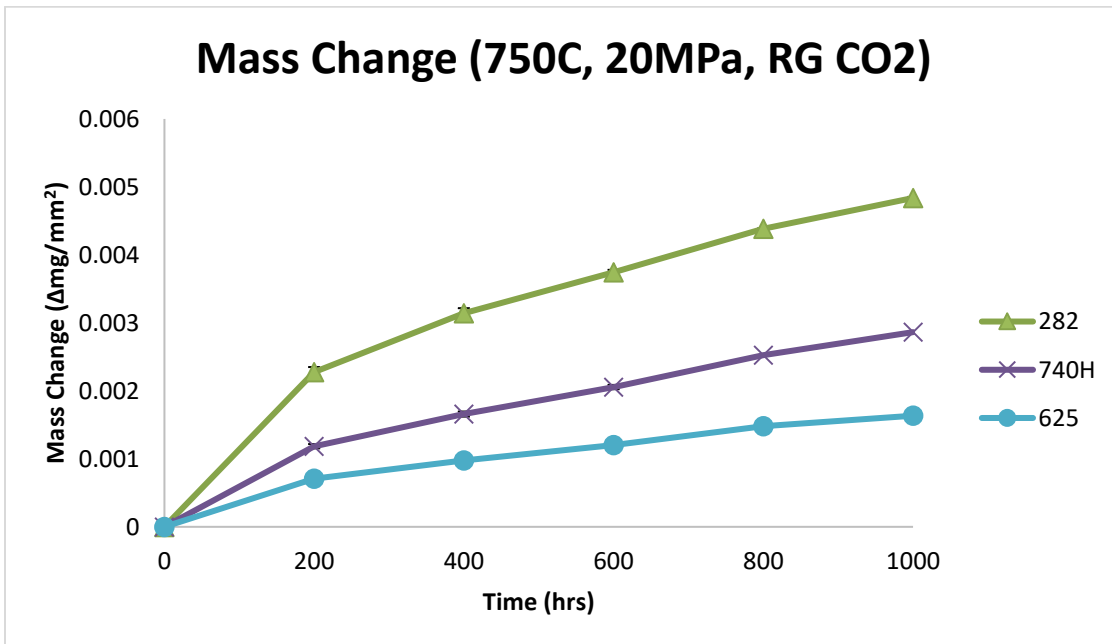


Figure 2 - Mass Chnge for Various Ni-base Alloys in RG CO<sub>2</sub> at 750°C, 20MPa (Mahaffey, 2017)

The recommended heat treatment procedure of both 740H and 282, in either the annealed or welded condition, is 800°C for a minimum of 4 hours, followed by air cooling. This allows for nucleation and growth of the  $\gamma'$ -phase, Ni<sub>3</sub>(Al,Ti,Nb), within the  $\gamma$ -matrix. While 800°C may be the optimal temperature for growth of  $\gamma'$ , aging at 750°C will continue to coarsen these precipitates. Given that 740H is currently code certified (282 is not), aging 740H at 750°C has been thoroughly studied. Two experiments, one by Yan and one by Guo, aged 740H for up to 10,000 hours and observed coarsening of both grains and  $\gamma'$  precipitates. Yan performed tensile tests at 750°C which found that yield strength (YS) had a maximum

at 500 hours, after which it decreased. Ultimate tensile strength (UTS) decreased steadily with aging time, while elongation increased. Transmission electron microscopy (TEM) was performed which observed a growth of  $\gamma'$  precipitates during aging, with the maximum YS corresponding to a mean precipitate diameter of 53.0nm (Yan, Zhengdong, Godfrey, Wei, & Yuqing, 2014).

Guo performed hardness tests after aging at 750°C and found a maximum in hardness at 300 hours of aging, after which it decreased. This 300 hours of aging corresponded to a mean  $\gamma'$  precipitate diameter of 47nm, determined by TEM (Guo, Li, Wang, Hou, & Wang, 2016). As the trend of hardness is correlated to that of the YS of a material, it is in good agreement with Yan that there is a maximum strength added from  $\gamma'$  corresponding to a critical precipitate diameter of roughly 50nm. As 282 and 740H are compositionally similar and both rely on  $\gamma'$  as a strengthening agent, it is hypothesized that their performance in CO<sub>2</sub> at 750°C may be similar.

### Experimental

740H and 282 material was provided and welded by the manufacturers, Special Metals and Haynes, respectively. Compositions of as-received material are provided in Table 1. Welded samples were produced through butt-welds by gas-tungsten arc welding of 1/8" thick plate. Samples consisting of purely base material and of welded sections were produced using EDM after standard heat treatments were applied. Both tensile samples, described below, and rectangular corrosion samples were produced – see Table 2 for the full list of tested samples.

	Cr	Co	Al	Ti	Nb	Fe	C	Mn	Mo	Si	W	Ni
740H (Base Samples)	24.57	20.09	1.33	1.33	1.46	0.1491	0.023	0.245	0.35	0.17	0.022	Bal
740H (Weld Samples)	24.56	20.02	1.37	1.47	1.52	0.2	0.036	0.3	0.503	0.15	0.046	Bal
740H (Filler Metal)	24.62	20.19	1.34	1.36	1.52	0.24	0.043	0.25	0.007	0.14	0.044	Bal
282 (Nominal)	20	10	1.5	2.1	---	1.5	0.06	0.3	8.5	0.15	---	Bal
282 (Weld Samples)	19.47	10.13	1.48	2.25	<0.1	0.79	0.065	0.08	8.58	<0.05	0.03	Bal
282 (Filler Metal)	19.43	10.42	1.50	2.16	<0.1	0.68	0.064	0.05	8.55	<0.05	0.002	Bal

Table 1 - Compositions of 740H and 282 used in this study

		740H		282	
		Base Material	Welded	Base Material	Welded
Unexposed	Tensile	5	3	3	4
	Corrosion	0	2	0	2
750C, CO <sub>2</sub>	Tensile	5	2	2	3
	Corrosion	0	2	0	2
750C, HT	Tensile	4	2	2	0
	Corrosion	0	2	0	4

Table 2 – Samples analyzed under each condition. Corrosion samples were used to analyze corrosion effect on fusion and heat affected zones relative to base material. Note: welded 282 samples were not prepared at the time of heat treatment exposure.

In order to properly compare base material and welded samples, the same tensile sample design was utilized for all samples. The dimensions of the tensile samples were designed in compliance with the ASTM standard with a slight elongation of the gauge to incorporate a maximum amount of the weld (Standard, 2013). The final tensile sample, shown in Figure 3, was designed with to fit inside an autoclave, including a 0.125 inch diameter hole to suspend the sample from a supporting alumina rod inside the autoclave during exposure. The tab with the hole was elongated to maintain sufficient surface area on each tab to ensure no slippage during tensile testing. The tensile samples were cut transversely in relation

to the weld with the gauge positioned to capture the fusion zone, heat affected zone (HAZ), and base material.

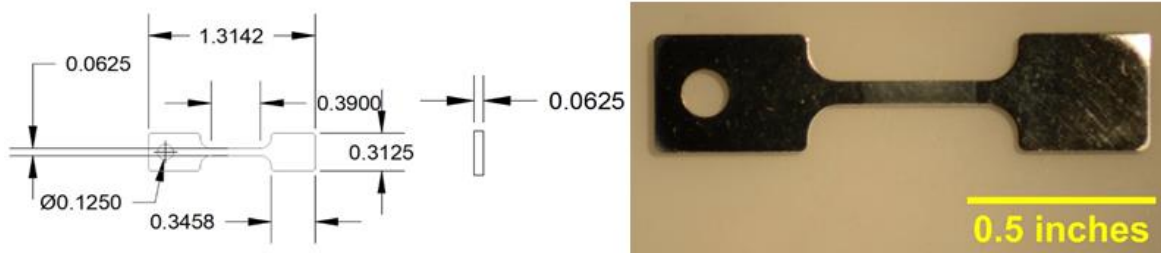


Figure 3 - Tensile specimen design (left) and etched 740H transverse weld tensile sample (right, with weld shown in center)

Samples were analyzed using a field emission scanning electron microscope (SEM) equipped with energy dispersive spectroscopy (EDS). Tensile testing was performed using a MTS QTest5 tensile machine with a 5kN load cell. Samples were tested in the unexposed (with standard heat treatments), sCO<sub>2</sub> exposed (RG CO<sub>2</sub> at 750°C, 20MPa for 1,000 hours), and heat treated (HT, argon at 750°C, 10MPa for 1,000 hours) conditions. Heat treatment was performed to better isolate the effect of thermal aging from that of exposure to sCO<sub>2</sub>. Etching of 282 was performed by immersing sample in HCl-1%H<sub>2</sub>O<sub>2</sub> for 10 seconds.

## RESULTS AND DISCUSSION

Exposure of samples of 740H and 282 to CO<sub>2</sub> at 750°C revealed worse corrosion performance in the welded samples for both materials relative to the samples of pure base material. No samples exhibited signs of spallation of the oxide on the surface, so the mass change results can be used as a good approximation for corrosion performance. As seen in Figure 4, welded samples of 740H and 282 exhibited a 23% and a 34% increase in mass gain, respectively. It should be noted that due to the welded samples being transverse and the inherent inhomogeneity of the welding process, welded samples are not entirely composed of fusion zone, but also the HAZ and base metal. This means that the ratios of fusion zone and HAZ to base material that is exposed to the environment is somewhat variable in each sample. The mass change is, therefore, understood qualitatively to have increased in the welded samples, but quantitative

analysis from this number is not informative. These results indicate that there is increased carbon and/or oxygen uptake inside the fusion zone.

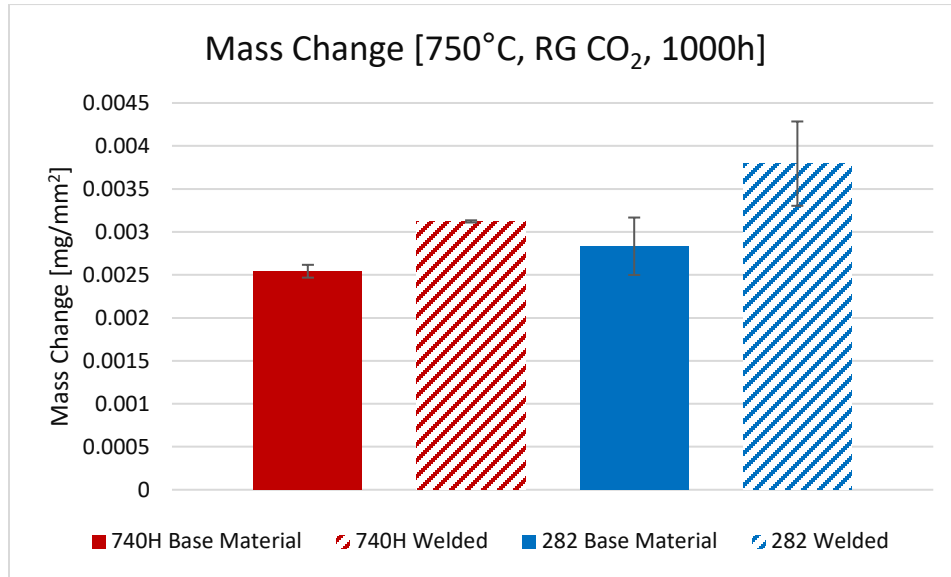


Figure 4 - Mass Change for 740H and 282 in RG CO<sub>2</sub> environment for 1,000 hours at 750°C, 20MPa

Tensile results for both base material and weld samples for 740H and 282 are given in Table 3. From literature, it is expected that both sCO<sub>2</sub>-exposure and heat treatment should increase the yield strength. In analyzing 740H, base material exposed to CO<sub>2</sub> gained approximately 7% in UTS and 5% in YS while suffering only a 31% loss of elongation relative to unexposed. However, HT samples exhibited no change in YS with a 53% drop in elongation relative to unexposed. The UTS remained relatively constant, indicating an increase in the stress required for plastic deformation. Welded samples appeared to respond somewhat differently than base material. For sCO<sub>2</sub>-exposed samples, UTS dropped by 11%, YS dropped by 17%, and elongation dropped by 54%. In contrast to that, the heat treated samples exhibited similar UTS, with decreases of 7% for YS, and 39% for elongation in relation to unexposed. Heat treated samples were largely unaffected by their exposures except to exhibit a drop in ductility. The sCO<sub>2</sub>-exposed samples experienced a very large drop in YS which combined with a drop in ductility to produce a much lower UTS. All welded samples appeared to fracture inside the fusion zone. Welded results are somewhat opposite of base material samples which experienced an increase in strength with only a moderate drop in elongation after exposure to sCO<sub>2</sub>. This indicates that welds – particularly the fusion zones – are the critical locations during long-term CO<sub>2</sub> exposure at 750°C.

	UTS (MPa)	0.2% YS (MPa)	Elongation (%)	Failure Location
<b>740H: Unexposed</b>	<b>1,111 ± 6</b>	<b>681 ± 3</b>	<b>38 ± 1.3</b>	<b>N/A</b>
<b>740H: 750C CO<sub>2</sub></b>	1,187 ± 2	713 ± 3	26 ± 0.5	N/A
<b>740H: 750C HT</b>	1,119 ± 22	673 ± 4	19 ± 2.0	N/A
<b>Welded 740H: Unexposed</b>	<b>1,068 ± 22</b>	<b>759 ± 16</b>	<b>26 ± 2.6</b>	<b>Fusion Zone</b>
<b>Welded 740H: 750C CO<sub>2</sub></b>	940 ± 10	638 ± 7	12 ± 2.0	Fusion Zone
<b>Welded 740H: 750C HT</b>	1,039 ± 4	710 ± 4	16 ± 1.0	Fusion Zone
<b>282: Unexposed</b>	<b>1,105 ± 15</b>	<b>728 ± 7</b>	<b>39.9 ± 0.4</b>	<b>N/A</b>
<b>282: 750C CO<sub>2</sub></b>	1,105 ± 9	741 ± 1	20.5 ± 1.0	N/A
<b>282: 750C HT</b>	1,052 ± 84	746 ± 18	13.0 ± 3.1	N/A

<b>Welded 282: Unexposed</b>	<b>867 ± 25</b>	<b>637 ± 11</b>	<b>10.1 ± 1.0</b>	<b>Fusion Zone</b>
<b>Welded 282: 750C CO<sub>2</sub></b>	<b>966 ± 5</b>	<b>684 ± 2</b>	<b>9.6 ± 0.5</b>	<b>Fusion Zone</b>

*Table 3 – Tensile results for 740H and 282 (base material and welded samples)*

The analysis of 282 base material samples showed a drop in elongation of 49% and 67% for sCO<sub>2</sub>-exposed and heat treated samples, respectively. There was a 2% increase in YS for both exposures, indicating a very slight hardening due to the aging process. There was no statistical change in UTS for either sCO<sub>2</sub>-exposed samples or heat treated samples. Welded samples exposed to CO<sub>2</sub> exhibited an increase of 11% in UTS and 7% in YS, with no statistical difference in elongation. It should be noted that the unexposed results for the 282 weld indicate the weld used for this experiment was of a quality that was acceptable to Haynes, but not optimal (Caron & Pike, 2014). However, the results of the 1,000 hour exposure at 750°C – similar to that of the initially higher quality 740H weld – indicate that the effects of embrittlement may not be proportional to initial properties but rather only restrict the maximum ductility of the weld. Additional testing with varying quality welds will need to be performed to confirm this theory, as the differing compositions of 740H and 282 mean the results are not directly comparable.

It has been shown that heat treatment of 740H at 750°C results in grain coarsening (Yan et al., 2014) and M<sub>23</sub>C<sub>6</sub> carbide formation along grain boundaries (Guo et al., 2016). Both effects individually decrease bulk ductility. Carbides including Cr<sub>23</sub>C<sub>6</sub> form along grain boundaries at 750°C, creating a chromium-denuded zone around the grain boundaries. While 740H has been shown to have a precipitate free zone (PFZ) along grain boundaries after standard post-weld heat treatment (DuPont, 2013), no PFZ was observed in 740H after exposure to CO<sub>2</sub> at 750°C for 1,000 hours, either inside or outside the fusion zone, see Figure 5 A,B. However, as observed in Figure 5 C and D, 282 was observed to have a PFZ on the order of 100nm surrounding any grain boundary carbides after 1,000 hours at 750°C. This effect was more pronounced inside the fusion zone, where carbides were present along all observable grain boundaries (only intermittently present in base material). The prevalence of brittle carbides along grain boundaries present in both materials lead to intergranular fracture in all tested samples. The differences in near-grain boundary phenomena governed the observed differences in fracture ductility.

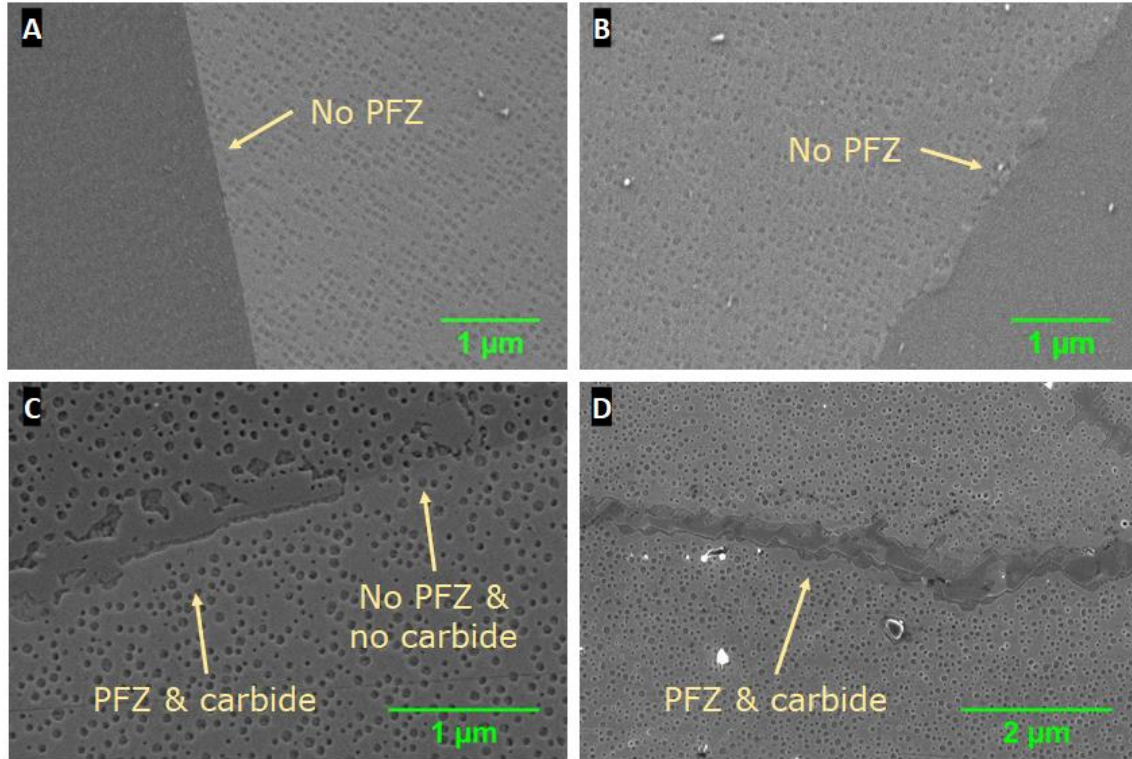


Figure 5 – SEM images of samples exposed to CO<sub>2</sub> at 750°C, 20MPa for 1,000 hours showing  $\gamma'$  precipitates approaching grain boundaries in a) 740H base material, B) 740H fusion zone, C) 282 base material, and D) 282 fusion zone. Images show a PFZ around carbides in 282, but not in 740H. Carbides are intermittent in 282 base material, while they are present along entirety of grain boundaries in fusion zone.

Intergranular failure can be observed in Figures 6-9 (A,B) after the standard heat treatment procedure was conducted. Fracture of 740H in the unexposed condition is characterized by intergranular micro-void coalescence (MVC) with dimples on the order of 10 $\mu$ m in diameter (see Figure 6 and Figure 7 B). Fracture surface of CO<sub>2</sub> exposed base material samples exhibit a mixture of micron-scale cleavage (likely due to intergranular carbides) and MVC with dimple size of roughly half that of the unexposed MVC, see Figure 6 D. Welded samples, meanwhile, also revealed MVC with reduced dimple size, but additionally had segments of grain boundary cracking in which grain boundaries sheared brittle enough to reveal the dendritic structure of the grains, see Figure 7 D. The embrittled fracture mechanism of the fusion zone is believed to be a result of the combination of grain boundary carburization and the lack of a PFZ, as seen in Figure 5 D.

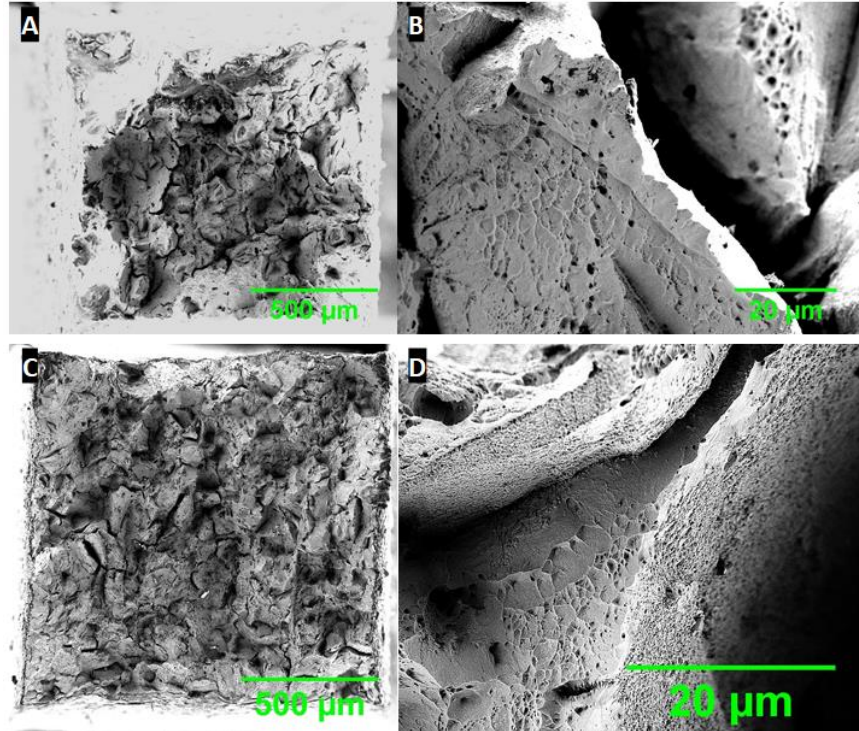


Figure 6 – 740H base material tensile sample fracture surfaces. Unexposed sample (A,B) and CO<sub>2</sub> exposed sample (C,D). Fracture is intergranular in both cases (A,C).

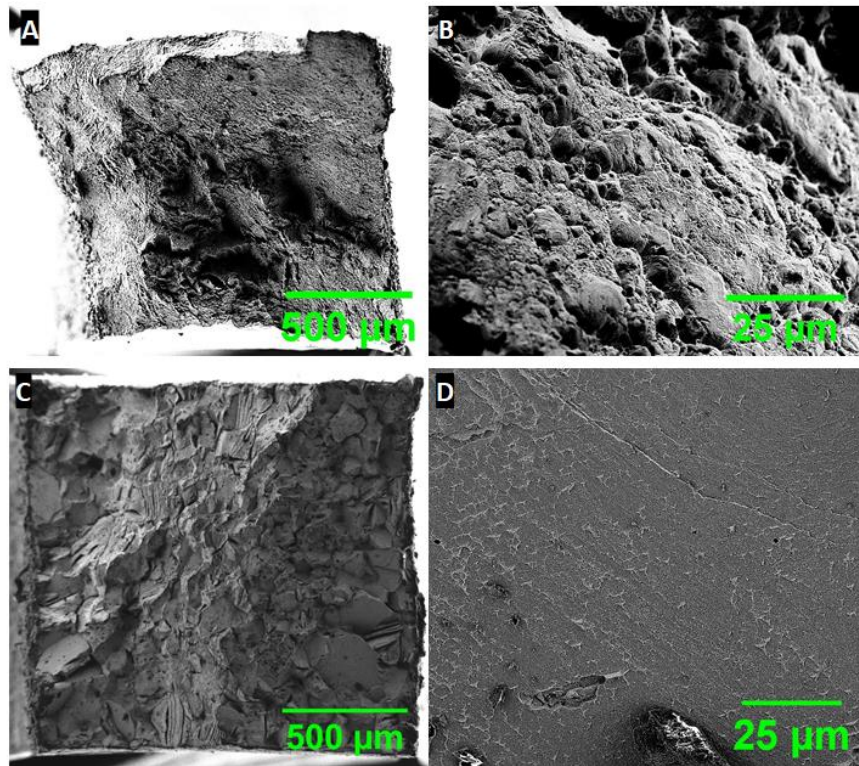


Figure 7 – 740H welded tensile sample fracture surfaces. Unexposed sample which fractured inside the fusion zone (A,B) and CO<sub>2</sub> exposed sample which fractured inside the fusion zone (C,D). Fracture is intergranular in both cases (A,C).

The effect of grain boundary embrittlement with aging was equally evident in 282. In the unexposed condition (experiencing only standard heat treatment procedures), 282 exhibited a fracture surface of MVC with micron-scale dimples in the base material case, see Figure 8 B, and a mixture of MVC and sub-micron-scale cleavage in the welded case, and Figure 9 B. After exposure, it can be seen in Figure 8 D that the base material is revealed to have failed with a mixture of MVC (similar-sized dimples to unexposed) and sub-micron-scale cleavage. In addition, exposed welded samples were found to fail with micron-scale cleavage, see Figure 9 D, with the size of the cleavage facets noticeably increasing in size. This is a sign of embrittlement and is likely due to coarsening of both the intergranular carbides and the corresponding PFZs. It was observed that no oxidation or carbide deposition occurred beyond a few microns at the surface due to the CO<sub>2</sub> environment. As a result of this, there was no observed difference in fracture mechanism between CO<sub>2</sub> and HT exposed samples after 1,000 hours. Fracture surface images of the HT samples were, therefore, omitted from this report.

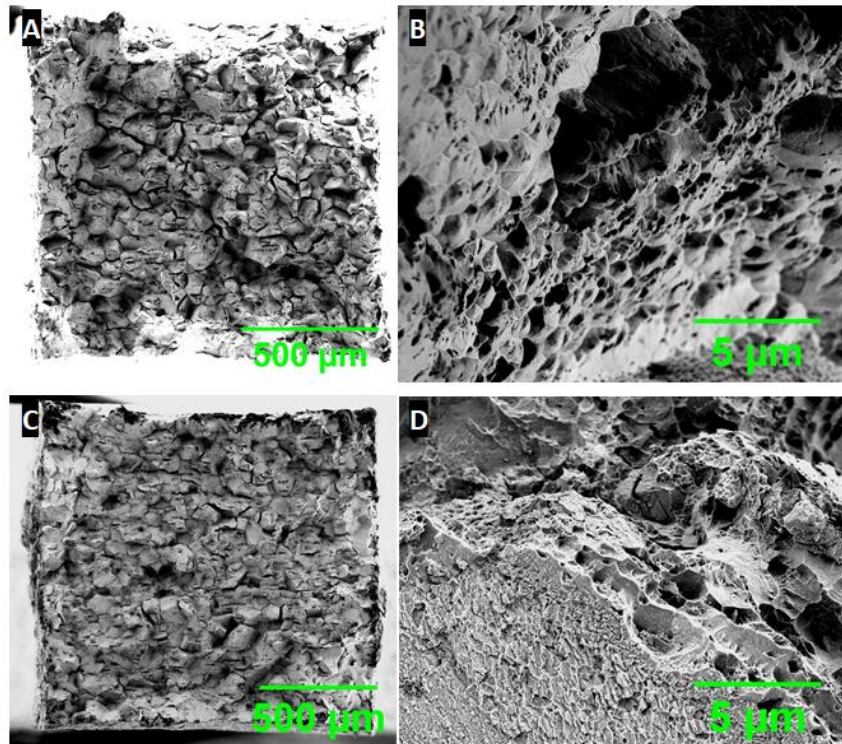


Figure 8 - 282 base material tensile sample fracture surfaces. Unexposed sample (A,B) and CO<sub>2</sub> exposed sample (C,D). Fracture is intergranular in both cases (A,C).

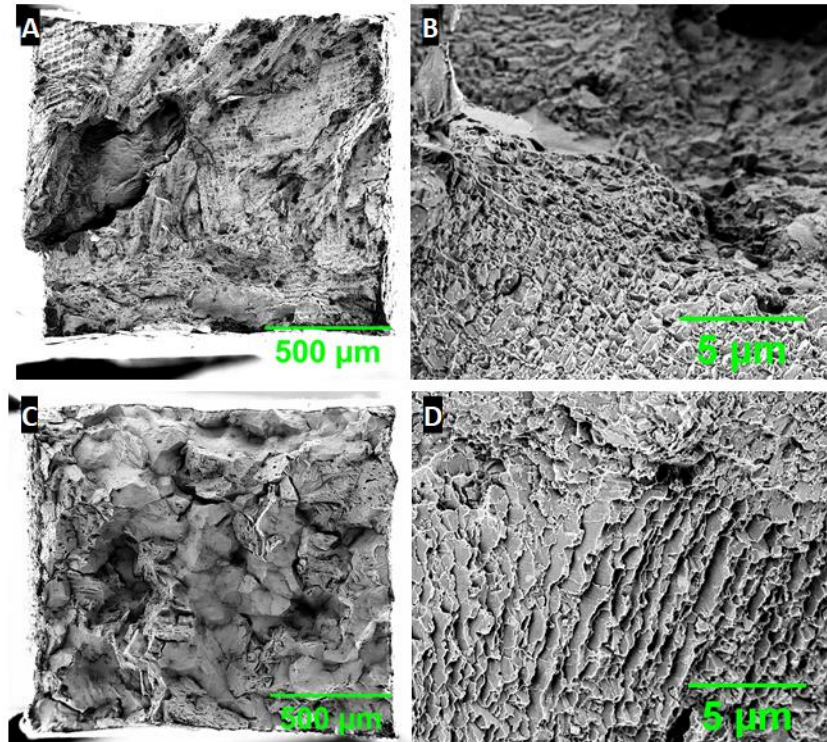


Figure 9 - 282 welded tensile sample fracture surfaces. Unexposed sample which fractured inside the fusion zone (A,B) and CO<sub>2</sub> exposed sample which fractured at the interface of the fusion zone and heat affected zone (C,D). Fracture is intergranular in both cases (A,C).

## Conclusions

Welded samples of 740H and 282 exposed to CO<sub>2</sub> at 750°C resulted in an increased corrosion rate of 23% and 34%, respectively, compared to base material. After exposure to CO<sub>2</sub>, 740H base material showed an increase in UTS of 7% and YS of 5% while experiencing a 31% drop in elongation relative to unexposed. This contrasts with 740H weld samples which exhibited a decrease in UTS (11%), YS (17%), and elongation (54%). 282 was less affected when exposed to the CO<sub>2</sub> environment. 282 Base material experienced a 2% increase in YS and a 49% decrease in elongation to result in a UTS which was not changed by CO<sub>2</sub> exposure. 282 transverse weld samples experienced an increase in UTS (11%), YS (7%), with no change in elongation. The 282 weld was initially of lower quality than that of 740H, so the gross mechanical properties of each weld after exposure to CO<sub>2</sub> was very similar despite the difference relative to unexposed. SEM revealed a PFZ around grain boundary carbides in 282 on the order of 100nm, but no observable PFZ along grain boundaries in 740H. Intergranular fracture occurred in all cases, with the fracture surface becoming more brittle after exposure at 750°C for 1,000 hours. No difference was observed in fracture mechanics between CO<sub>2</sub> exposure and neutral environment heat treatment, and no oxygen or carbon deposition occurred due to the environment beyond a few microns of the surface. This work indicates that welds of 740H and 282 will be the primary locations for potential failure in industrial pressure vessels (known), and additionally that the CO<sub>2</sub> environment does not negatively affect the bulk mechanical properties of these alloys.

## REFERENCES

Boiler and Pressure Vessel Code: Section II Part D. (2013). New York: The American Society of Mechanical Engineers.

Caron, J., & Pike, L. (2014). Weldability of HAYNES 282 Superalloy After Long-Term Thermal Exposure.

*MATEC Web of Conferences*, 14. <http://doi.org/10.1051/mateconf/20141413003>

- Dostal, V. (2004). *A Supercritical Carbon Dioxide Cycle for Next Generation Nuclear Reactors*. Massachusetts Institute of Technology.
- DuPont, J. N. (2013). Welding of Nickel-Based Alloys for Energy Applications. *Welding Journal*, 93(February), 31–45.
- Guo, Y., Li, T., Wang, C., Hou, S., & Wang, B. (2016). Microstructure and phase precipitate behavior of Inconel 740H during aging. *Transactions of Nonferrous Metals Society of China*, 26(6), 1598–1606. [http://doi.org/10.1016/S1003-6326\(16\)64266-8](http://doi.org/10.1016/S1003-6326(16)64266-8)
- Mahaffey, J. T. (2017). *Effect of Partial Pressure of Oxygen and Activity of Carbon on the Corrosion of High Temperature Alloys in s-CO<sub>2</sub> Environments*. University of Wisconsin-Madison.
- Standard, A. S. T. M. (2013). *Standard Test Methods for Tension Testing of Metallic Materials E8/E8M*. West Conshohocken, PA: ASTM International. <http://doi.org/10.1520/E0008>
- Yan, C., Zhengdong, L., Godfrey, A., Wei, L., & Yuqing, W. (2014). Microstructure Evolution and Mechanical Properties of Inconel 740H During Aging at 750C. *Materials Science & Engineering A*, 589, 153–164. <http://doi.org/10.1016/j.msea.2013.09.076>

## ACKNOWLEDGEMENTS

The author gratefully acknowledges that this work would not have been completed without funding from Advance supercritical carbon dioxide cycles DE-EE0007120 and the U.S. Department of Energy. The author further acknowledges the contributions to the work made by Brian Baker and Ronald Gollihue of the Special Metals Corporation, Vinay Deodeshmukh and Jeremy Caron of Haynes International, as well as John Shingledecker and John Siefert of the Electric Power Research Institute. Finally, a special thanks to Ryan Carroll and Peter Li who performed significant work in completing this research.